Bull. Chem. Soc. Jpn., **68**, 1036—1041(1995)

Effect of an Oxygen-Binding Reaction at the Cobalt Porphyrin Site Fixed in a Polymer Membrane on Facilitated Oxygen Transport

Takayuki Suzuki, Yuji Soejima, Hiroyuki Nishide,* and Eishun Tsuchida*

Department of Polymer Chemistry, Waseda University, Shinjuku, Tokyo 169

(Received October 5, 1994)

Oxygen transport was facilitated in polymer membranes bonded with new derivatives of [*meso*-$\alpha,\alpha,\alpha,\alpha$-tetrakis(*o*-pivalamidophenyl)porphyrinato]cobalt (CoPs). The oxygen-binding reactivity of fixed CoPs strongly influenced the facilitated oxygen transport. CoP having a larger cavity structure showed a more rapid reactivity and achieved a higher oxygen permeability in the membrane. There existed correlations of the oxygen-binding and -dissociation rate constants with the diffusion constant of oxygen via CoPs fixed in the membrane.

Facilitated transport is a process used to selectively augment the permeation rate of a specific component in a feed stream relative to all other components by means of a carrier molecule forming a chemical adduct with the specific component in a membrane.[1,2] We have demonstrated this facilitate transport by using solid polymer membranes containing metalloporphyrins;[3—5] the metalloporphyrins fixed in the membranes acted as a fixed carrier of oxygen and facilitated the transport of oxygen relative to nitrogen. These metalloporphyrin membranes are expected to allow high oxygen/nitrogen permselectivity.

The facilitated oxygen transport in a solid membrane containing a fixed carrier involves the chemically specific absorption process of oxygen (oxygen-binding reaction) on the feed side of the membrane, the diffusing process of oxygen which repeats the oxygen-binding and -dissociation reaction via the fixed carrier, and the stripping process (oxygen-dissociation reaction) on the product or permeate side of the membrane. An analysis of the correlation between the oxygen-binding reactivity in the membrane and the facilitated oxygen permeability through the membrane is expected to produce a highly oxygen-permeable membrane. We analyzed the facilitated oxygen transport in metalloporphyrin polymer membranes using a modified dual-mode transport model.[5] We also reported on the effect of the oxygen-binding and -dissociation rate constants of the metalloporphyrin carriers fixed in membranes on the diffusion constant of oxygen in the membranes; a higher oxygen-binding reactivity contributes to a more efficient facilitation of oxygen in the membrane.[6,7]

This paper describes the correlation of the oxygen-binding and -dissociation rate constants of cobalt porphyrins (CoPs) fixed in a polymer membrane and the facilitated oxygen transport after preparing new CoPs as oxygen carries (Chart 1) with a large cavity structure over the porphyrin plane. The following three new CoP derivatives of the well-known [*meso*-$\alpha,\alpha,\alpha,\alpha$-tetrakis(*o*-pivalamidophenyl)porphyrinato]cobalt(II) (CoB_4P) were prepared: [*meso*-β-(*o*-acetamidophenyl)-α,α,α-tris(*o*-acetamidophenyl)porphyrinato]cobalt(II) (CoM_3P), [*meso*-β-(*o*-acrylamidophenyl)-α,α,α-tris(*o*-acrylamidophenyl)porphyrinato]cobalt(II) (CoE_3P), and [*meso*-β-(*o*-pivalamidophenyl)-α,α,α-tris(*o*-pivalamidophenyl)porphinato]cobalt(II) (CoB_3P). We measured both the oxygen-binding reaction spectroscopically and the permeation of oxygen and nitrogen through the membranes in order to determine the equilibrium and rate constants for the oxygen-binding of CoPs bonded to and fixed in the solid poly(octyl methacrylate-*co*-1-vinylimidazole), and the oxygen solubility coefficient and oxygen-diffusion constants in the membranes, respectively. Poly(octyl methacrylate-*co*-1-vinylimidazole) is adequate as a membrane material due to its rubbery property with a T_g of −10 °C. We report on the correlation of the oxygen-binding reactivity of the fixed CoP and the oxygen diffusivity in the membrane.

Experimental

Materials. *meso*-β-(*o*-Acetamidophenyl)-α,α,α-tris(*o*-acetamidophenyl)porphyrin (H_2M_3P) was prepared as follows. Acetyl chloride was added at 0—5 °C to a chloroform solution of *meso*-β-(*o*-aminophenyl)-α,α,α-tris(*o*-aminophenyl)porphyrin, which was separated on a silca-gel column using chloroform/diethyl ether (4/1 v/v) as the eluent ($R_f = 0.40$) from a mixture of its atropisomers,[8] purchased from Satoh Yakugaku Inc.. The product was purified by chromatography on a silica-gel column using chloroform/acetone (2/1 v/v) as the eluent ($R_f = 0.44$). ^{1}H NMR

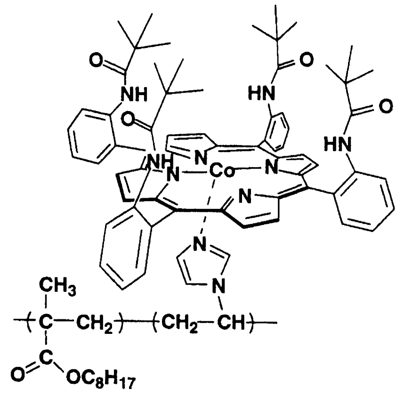

CoB_4P

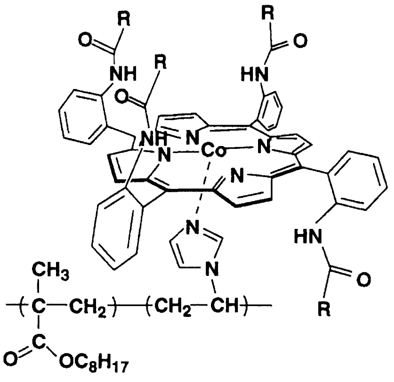

R ;	$-C(CH_3)_3$	CoB_3P
	$-CHCH_2$	CoE_3P
	$-CH_3$	CoM_3P

Chart 1.

($CDCl_3$) $\delta = -2.7$ (2H, inner-H), 1.65, 1.75, 1.8 (12H, $-CH_3$), 7.1—7.9 (16H, phenyl-H), 8.7 (4H, amino-H), 8.8 (8H, pyrrole-H). UV-vis λ_{max} 642, 588, 547, 515, and 423 nm in toluene. Cobalt insertion was carried out by refluxing the methanol/chloroform (1/1 v/v) solution of H_2M_3P and cobaltous acetyl acetate as described in the literature.[9] UV-vis λ_{max} (after the cobalt insertion) 529, 412 nm in toluene.

meso-*β*-(*o*-Acrylamidophenyl)-*α*,*α*,*α*-tris(*o*-acrylamidophenyl)porphyrin was prepared by reacting acryloyl chloride in a manner similar to H_2M_3P. The product was purified by chromatography on a silica-gel column using chloroform/acetone (10/1 v/v) as the eluent ($R_f = 0.27$). ^{1}H NMR ($CDCl_3$) $\delta = -2.7$ (2H, inner-H), 5.0, 5.05, 5.1 (8H, $-CH{=}C\underline{H}_2$), 5.8, 5.9, 6.0 (4H, $-C\underline{H}{=}CH_2$), 7.1—7.9 (16H, phenyl-H), 8.6 (4H, amino-H), 8.9 (8H, pyrrole-H). UV-vis λ_{max} 642, 586, 545, 514, and 421 nm in toluene. UV-vis λ_{max} (after cobalt insertion) 529, 412 nm in toluene.

meso-*β*-(*o*-Pivalamidophenyl)-*α*,*α*,*α*-tris(*o*-pivalamidophenyl)porphyrin was also prepared by reacting pivaloyl chloride. The product was purified on a silica-gel column using cyclohexane/ethyl acetate (3/2 v/v) as the eluent ($R_f = 0.40$). ^{1}H NMR ($CDCl_3$) $\delta = -2.72$ (2H, inner-H), 0.10, 0.16, 0.21 (36H, $-C(CH_3)_3$), 7.2—7.9 (16H, phenyl-H), 8.6 (4H, amino-H), 8.8 (8H, pyrrole-H). UV-vis λ_{max} 644, 588, 547, 514, and 429 nm in toluene. UV-vis λ_{max} (after cobalt insertion) 525, 411 nm in toluene.

[*meso*-*α*,*α*,*α*,*α*-tetrakis(*o*-Pivalamidophenyl)porphyrinato]cobalt(II) (CoB_4P) was synthesized as previously described in the literature.[10]

Poly(octyl methacrylate-*co*-1-vinylimidazole) was prepared by radical copolymerization of octyl methacrylate and 1-vinylimidazole initiated by azobis(isobutyronitrile). The molecular weight and vinylimidazole residue content of the copolymer were determined to be 1.7×10^6 and 3.3 mol%, by gel permeation chromatography (with tetrahydrofuran used as the solvent and polystyrene as the standard) and an elemental analysis, respectively. Chloroform solutions of the copolymer and CoP were mixed so as to combine the vinylimidazole residue of the copolymer with the fifth coordination site of CoP. The solution was carefully cast on a Teflon® plate under an oxygen-free atmosphere followed by drying in vacuo to yield a transparent, red-colored membrane having a thickness of 90 µm and containing 1.3 wt % CoP. The fixed and active amounts of oxygen in the membrane were measured using a sorption apparatus (Makuhari Kagaku KA-102).

Spectroscopic and Permeation Measurements. Bonding of CoP with the imidazole residue in poly(octyl methacrylate-*co*-1-vinylimidazole) and oxygen-binding to the CoP fixed in the solid membrane were measured by a spectral change in its visible absorption using a spectrophotometer (Shimadzu Model UV-2100). ESR spectroscopy of the oxygen adduct of CoP in the membrane was measured with a JEOL RE-2X ESR spectrometer operating in the X-band at 110 and 210 K, after setting the membrane piece in a glass tube. The magnetic fields were corrected with the splitting of Mn(II) in MnO ($\Delta H = 86.9$ G).

Pulsed laser-flash irradiation was perpendicularly applied to the membrane to the light path of the spectrophotometer (Unisoku FR-2000), as previously reported in the literature.[7] Monitoring wavelengths of 411 and 428 nm were selected, which agreed with the maxima of the deoxy- and oxy-CoP, respectively. The oxygen-binding and -dissociation rate constants were calculated by a pseudo-first-order kinetic analysis in the time courses at these absorbances. The concentration of oxygen in the membrane was calculated using the oxygen solubility coefficient determined by a permeation measurement.

The oxygen and nitrogen permeation coefficients for various upstream oxygen/nitrogen pressures were measured with a low-vacuum permeation apparatus in a chamber equipped with a stable thermostat (Rika Seiki K-315N-03). The pressures on the upstream and the downstream sides were detected using a Baratron absolute-pressure gauge (MKS Instruments). The permeation coefficients were calculated from the slopes of the steady state straight line sections of the permeation curves.

Results and Discussion

Bonding of the Imidazole Residue to Cobalt Porphyrins. A base ligand bonding to the fifth site of CoP is essential for the oxygen-binding capability of CoP. Many studies concerning chemical modification of CoPs based on CoB_4P (Collman's "picket-fence" metalloporphyrin)[11] showed that the cavity structure over the porphyrin plane affects both the bonding of a base ligand at the fifth site of CoP and binding of molecular oxygen at the sixth.[12—16)]

$$\mathrm{CoP} + \mathrm{Im} \overset{K^{\mathrm{b}}}{\rightleftharpoons} \mathrm{CoP\text{-}Im}. \qquad (1)$$

The equilibrium constant (K^{b}) for the bonding reaction of a base ligand with CoPs (Eq. 1) was estimated for an imidazole residue (Im) composing poly(octyl methacrylate-*co*-1-vinylimidazole) by measuring the visible absorbance at 527 nm ascribed to CoP-Im in the CoP membrane containing Im at various concentrations. The enthalpy and entropy changes (ΔH^{b}, ΔS^{b}) for the bonding reaction were also calculated from the dependence of K^{b} on the temperature, and are given in Table 1. The K^{b} values of new $\alpha^3\beta$-type CoPs are larger than that of α^4-type CoB_4P. An interaction of the β-amido group and the bonded Im may increase K^{b}. The largest K^{b} value for CoM_3P of all the new CoPs would be explained by a steric hindrance of the bulky β-amino group against the bonded Im.

Oxygen-Binding Reaction at Cobalt Porphyrins Fixed in Membranes. The oxygen binding to CoPs fixed in membranes was detected by ESR and the visible spectra. Slightly rhombic distorted and eight-line hyperfine splitted ESR spectra indicated the formation of the oxygen adduct of the CoP bonded to the polymer (1/1 O_2/CoP): e.g., $g_{//}=2.08$, $g_{\perp}=1.97$, $A^{\mathrm{Co}}_{//}=18.7$ G, $A^{\mathrm{Co}}_{\perp}=6.6$ G, ascribed to the O_2-CoP-Im. The visible spectrum of the membrane containing the deoxy CoP ($\lambda_{\max}=528$ nm) was changed to the spectrum of the corresponding oxy (oxygen-adduct) CoP ($\lambda_{\max}=547$ nm) with isosbestic points at 480, 538, and 667 nm. This oxy-deoxy spectral change in the membrane was rapid and reversible.

The equilibrium constant (K (cm Hg^{-1})) of the oxygen-binding reaction to the CoP fixed in the membrane (Eq. 2) was converted to K (M^{-1}) by substituting the solubility coefficient of oxygen in the membrane (Table 1) (1 M=1 mol dm^{-3}). The K values of the new CoPs are smaller than that of CoB_4P. ΔH or the enthalpy gain through the oxygen binding is also smaller for these CoPs (Fig. 1). The $\alpha^3\beta$-cavity structure reduces the oxygen-binding affinity of CoP.

$$O_2 + \mathrm{CoP\text{-}Im} \underset{k_{\mathrm{off}}}{\overset{k_{\mathrm{on}}}{\rightleftharpoons}} O_2\text{-}\mathrm{CoP\text{-}Im}, \ K = k_{\mathrm{on}}/k_{\mathrm{off}}. \qquad (2)$$

A rapid and reversible oxygen binding of CoP fixed in the polymer membrane was observed by laser flash photolysis. The positive and negative extremes in the differential spectrum, 411 and 428 nm, agreed with the absorption maxima of the deoxy- and the oxy-CoP. The absorbance at 418 nm was not changed either before or after flash irradiation, which coincided with the isosbestic point of the oxy- and deoxy-spectrum. The oxygen-binding and -dissociation rate constants (k_{on} and k_{off}, respectively) were estimated using the pseudo-first-order kinetics shown in Fig. 2, and are given in Table 1. The k_{on} value increases along with a reduction in the bulkiness in the substituent group on the porphyrin plane or in the oxygen-binding cavity in the order $CoM_3P > CoE_3P \gg CoB_3P > CoB_4P$. The k_{off} value increases in the same order: $CoM_3P > CoE_3P \gg CoB_3P \gg CoB_4P$. Especially, the k_{on} and k_{off} values of CoM_3P are ca. 120- and 600-times larger than those of CoB_4P, respectively. This means that these CoPs with a larger cavity structure over the porphyrin plane display a much higher kinetic activity for oxygen binding.

Facilitated Oxygen Transport through Polymer Membranes Containing Cobalt Porphyrins. The permeation time courses for membranes contain-

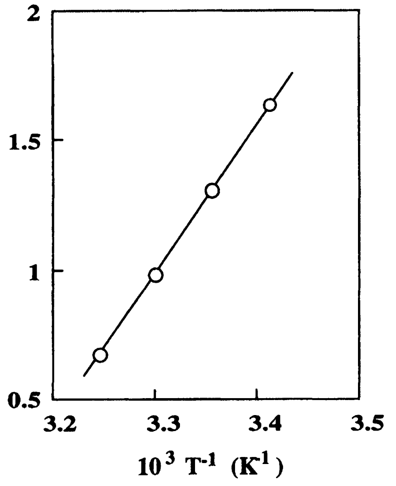

Fig. 1. van't Hoff plots (ln K vs. T^{-1}) for the membrane containing CoB_3P. K; cmHg^{-1}

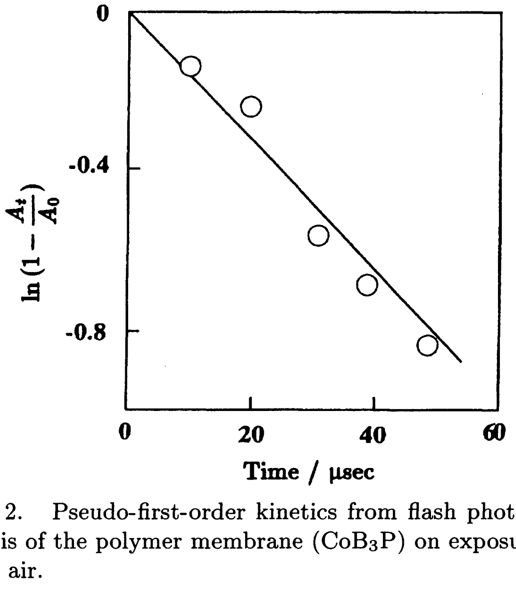

Fig. 2. Pseudo-first-order kinetics from flash photolysis of the polymer membrane (CoB_3P) on exposure to air.

Table 1. Equilibrium Constant for the Bonding Reaction of a Base Ligand with CoP (25 °C) and Rate Constants of Oxygen-Binding Reaction and Thermodynamic Parameters for the Polymer Membranes Containing CoP (45 °C)

CoP	10^{-4} K^{b}	ΔH^{b}	ΔS^{b}	10^{-2} K	ΔH	ΔS	10^{-7} k_{on}	10^{-6} k_{off}
	M^{-1}	kcal mol^{-1}	eu	M^{-1}	kcal mol^{-1}	eu	M^{-1} s^{-1}	s^{-1}
CoM3P	4.1	−9.4	−11	2.0	−12	−39	290	15
CoE3P	4.0	−9.4	−11	2.0	−12	−39	180	8.9
CoB3P	2.6	−9.7	−11	1.8	−11	−36	4.4	0.24
CoB4P	1.3	−11	−17	10	−13	−37	2.4	0.024

ing CoP reached steady-state straights lines, whose slopes determined the permeation coefficients (P). Before the steady state, there was an induction period. The time lag (θ) was estimated from the crossing point of the steady-state straight line and the abscissa on the permeation curve. The θ values for oxygen and nitrogen permeation (θ_{O2} and θ_{N2}) are shown in Fig. 3 vs. the upstream oxygen and nitrogen pressure ($p_2(O_2)$ and $p_2(N_2)$). While θ_{N2} is short and independent of $p_2(N_2)$, θ_{O2} is longer than θ_{N2}, and increases along with a decrease in $p_2(O_2)$. On the other hand, for a control membrane containing inactive Co(III)M3P for oxygen binding, θ_{O2} is also short and independent of $p_2(O_2)$. The fixed CoP in the membrane specifically interacts with oxygen and retards the diffusion of oxygen through the membrane. θ_{O2} decreases in the order CoB4P$\gg$CoB3P$>$CoE3P$>$CoM3P, which agrees with the oxygen-binding reactivity or rate constants of these CoPs.

Figure 4 shows the permeation coefficients of oxygen

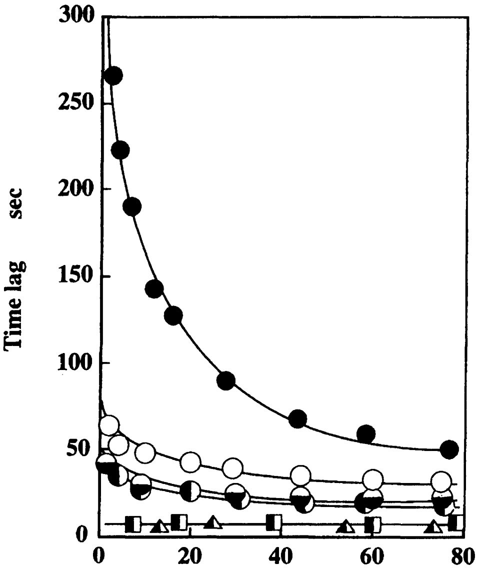

Fig. 3. Effect of upstream gas pressure on the time lag of the permeation for the CoP polymer membranes at 45 °C. Oxygen: (◒) CoM3P, (◐) CoE3P, (○) CoB3P, (●) CoB4P, (▲) inactive (control) Co^{III}M3P. Nitrogen: (□) CoM3P.

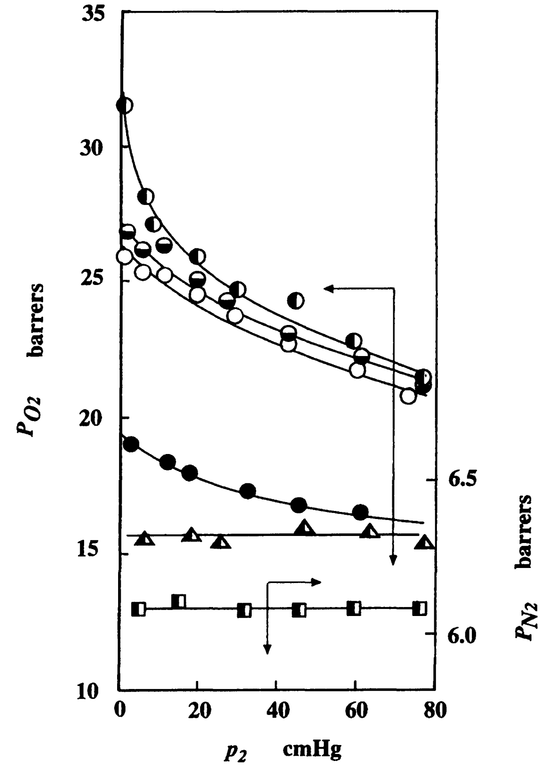

Fig. 4. Effect of upstream gas pressure on the permeability coefficient for the CoP polymer membranes at 45 °C. Oxygen: (◒) CoM3P, (◐) CoE3P, (○) CoB3P, (●) CoB4P, (▲) inactive (control) Co^{III}M3P. Nitrogen: (□) CoM3P.

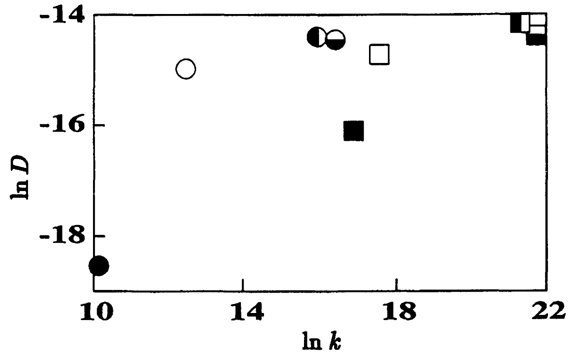

Fig. 5. Correlation of the diffusion constants of oxygen via CoP and the rate constants of oxygen-binding and -dissociation at 45 °C. and ln D_{CD} vs. ln k_{off}, ln D_{DC} vs. ln k_{on}; (◒,⬓) CoM3P, (◐,◧) CoE3P, (○,□) CoB3P, (●,■) CoB4P.

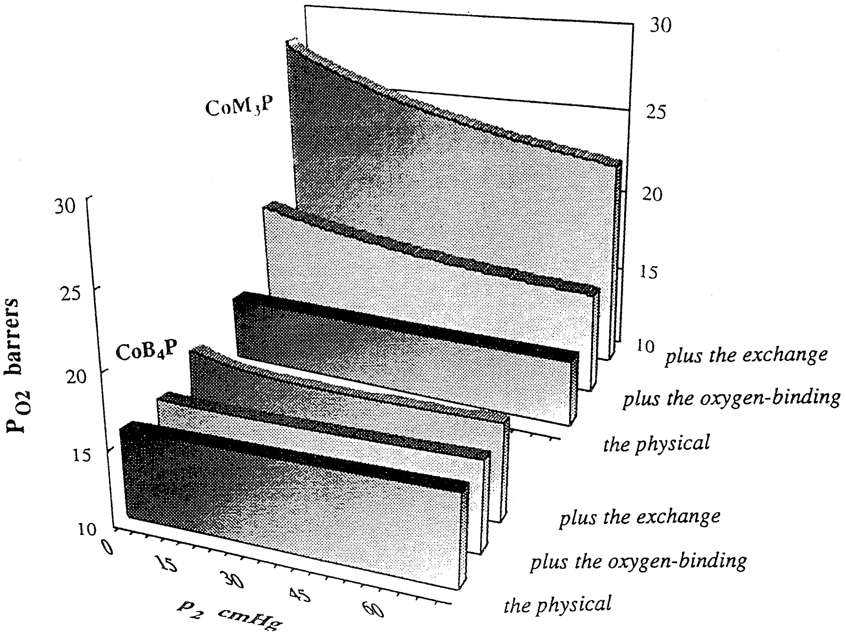

Fig. 6. Contribution of each mode in the modified dual-mode model to the total permeability coefficients for the CoM3P and CoB4P polymer membranes at 45 °C.

and nitrogen (P_{O2} and P_{N2}) for CoP membranes. P_{N2} is smaller than P_{O2} and is independent of $p_2(N_2)$, because the fixed CoP does not bind with nitrogen. In contrast, P_{O2} is larger than P_{N2} and increases with a decrease in $p_2(O_2)$, indicating that the fixed CoP carrier in the solid polymer membrane clearly interacts with oxygen and facilitates oxygen transport in the membrane. P_{O2} for a control membrane containing inactive Co(III)M3P is not enhanced at low $p_2(O_2)$. One notices that the P_{O2} values for membranes containing the new CoPs significantly increase at low $p_2(O_2)$ more than for the CoB4P membrane in Fig. 4. Higher kinetic activity in the oxygen binding of the new CoPs significantly enhances the facilitation of oxygen transport.

Analysis of Facilitated Oxygen Transport. We analyzed this facilitated transport in CoP membranes using a modified dual-mode transport model,[17,18)] as represented by the following equation:

$$P_{O2} = k_D D_{DD} + \frac{C_C' K D_{CC}}{(1+Kp_2)} + \left[\frac{C_C' K D_{CD} - k_D D_{DC}}{(1+Kp_2)} + \frac{2k_D D_{DC}}{(Kp_2)}\ln(1+Kp_2)\right], \quad (3)$$

where k_D is the physical solubility coefficient of oxygen in a polymer matrix. P_{O2} is the sum of the first term representing the physical oxygen permeation through a polymer matrix, the second term representing the oxygen-binding mode, i.e., a specific absorption and permeation of oxygen by and via the fixed CoP, and the third term representing the exchanging mode between the first and the second modes. D_{DD}, D_{DC}, D_{CD}, and D_{CC} are the diffusion constants of oxygen for the physical diffusion in the polymer membrane, for diffusion from the polymer matrix to the fixed CoP, for diffusion from the fixed CoP to the polymer matrix, and for hopping diffusion through CoP, respectively.

Each value of P_{O2} for membranes containing various inactive Co(III)Ps was the same, 16 barrers, approximately independent of CoP species. D_{DD} is calculated to be 10^{-6} cm^2 s^{-1} from a measurement of the induction period before the steady state of oxygen permeation for inactive CoP membranes, which agreed with the previously reported diffusion constants of oxygen in rubbery polymers.[6)] Therefore, not only D_{DD}, but also k_D, are not influenced by the CoP species or the porphyrin structure. The experimental date given in Fig. 4 were analyzed using Eq. 3, besides those k_D and D_{DD} values; the parameters for oxygen transport through the membranes given by a modified dual-mode transport model are listed in Table 2.

On the other hand, D_{DC}, D_{CD}, and D_{CC} involving oxygen diffusion via the fixed CoP carrier are smaller than D_{DD} and depend on the CoP species or the oxygen-binding character of CoP. Table 2 especially indi-

Table 2. Diffusion Constants of Oxygen in a Modified Dual-Mode Transport Model for the CoP Polymer Membranes at 45 °C

CoP	Diffusion constants (cm^2 s^{-1})			
	$10^6 D_{DD}$	$10^7 D_{DC}$	$10^7 D_{CD}$	$10^7 D_{CC}$
CoM3P	1.9	6.4	5.5	5.3
CoE3P	1.9	7.1	5.7	5.4
CoB3P	2.1	4.0	3.3	1.1
CoB4P	2.2	0.97	0.087	0.031

$10^4 k_D$ (cm^3(STP)cm^{-3}cmHg^{-1})=7.2; C'_C (cm^3(STP)cm^{-3})=0.2 for CoB4P, CoB3P, 0.1 for CoM3P, CoE3P; the CoP concentration in the membrane, 1.3 wt%.

cates that D_{CD} and D_{CC} are very large for membranes containing the new CoPs. A comparison of the diffusion constants of oxygen in Table 2 with the rate constants of oxygen-binding in Table 1 shows correlations of $\ln D$ and $\ln k$ of the CoPs in the membranes. In Fig. 5, $\ln k_{on}$ correlates with $\ln D_{DC}$ (square plots), and $\ln k_{off}$ with $\ln D_{CD}$ (circle plots). D_{CC} is related to both k_{on} and k_{off}; especially k_{off} clearly reflects D_{CC}. A polymer membrane containing CoP with large rate constants for oxygen-binding and -dissociation leads to a large diffusion constant to produce oxygen permselectivity or facilitated oxygen transport.

Figure 6 shows the contribution of each transport mode in Eq. 3 to the permeation coefficient by using the membrane examples of CoM_3P and CoB_4P. The P_{O2} attributed to the physical mode or the first term of Eq. 1 is almost equivalent to each other, because the concentration of CoP in the membrane and polymer species were the same. The most important parameter among these factors in the oxygen transport is the diffusion constants of oxygen via CoP. The diffusion constants (D_{CC}, D_{DC}, and D_{CD}) for oxygen binding and the exchange mode or the second and third terms in Eq. 1 augment P_{O2} or the facilitated transport of oxygen over a wide range of $p_2(O_2)$. Since the oxygen-binding and -dissociation rate constants of CoM_3P are extremely large, the D_{CC} value becomes comparable to the exchanging diffusion constants (D_{DC} and D_{CD}). The contribution of the third exchanging mode is almost twice the second oxygen-binding mode in the CoM_3P membrane and enhances the total P_{O2} value.

This work was partially supported by a Grant-in-Aid for Scientific Research No. 04453109 from the Ministry of Education, Science and Culture.

References

1) P. F. Scholader, *Science*, **131**, 585 (1960).

2) H. Nishide and E. Tsuchida, "Polymers for Gas Separation," ed by N. Toshima, VCH Publishers, New York (1992), pp. 183—219.

3) H. Nishide, M. Ohyanagi, O. Okada, and E. Tsuchida, *Macromolecules*, **20**, 417 (1987).

4) H. Nishide, H. Kawakami, Y. Kurimura, and E. Tsuchida, *J. Am. Chem. Soc.*, **111**, 7175 (1989).

5) H. Nishide, H. Kawakami, T. Suzuki, Y. Azechi, Y. Soejima, and E. Tsuchida, *Macromolecules*, **24**, 6306 (1991), and references cited therein.

6) H. Nishide, H. Kawakami, T. Suzuki, Y. Azechi, and E. Tsuchida, *Macromolecules*, **23**, 3714 (1990).

7) H. Nishide, T. Suzuki, H. Kawakami, and E. Tsuchida, *J. Phys. Chem.*, **98**, 5084 (1994).

8) J. Lindsey, *J. Org. Chem.*, **45**, 5215 (1980).

9) J. P. Collman, J. I. Brauman, K. M. Coxsee, T. R. Halbert, S. E. Hayes, and K. S. Suslick, *J. Am. Chem. Soc.*, **100**, 2761 (1978).

10) J. P. Collman, R. R. Gagne, C. A. Reed, J. R. Halbert, G. W. Lang, and T. Robinson, *J. Am. Chem. Soc.*, **97**, 1427 (1975).

11) J. P. Collman, *Acc. Chem. Res.*, **10**, 265 (1977).

12) M. J. Carter, P. P. Rillema, and F. Basolo, *J. Am. Chem. Soc.*, **96**, 392 (1974).

13) C. K. Chang, *J. Macromol. Sci., Chem.*, **A25**, 1307 (1988).

14) M. Momentoeu, B. Loock, C. Tetreau, D. Lavalette, A. Croisy, C. Schaeffer, C. Huel, and J. M. Lhoste, *J. Chem. Soc., Perkin Trans. 2*, **1986**, 249.

15) E. Tsuchida and H. Nishide, *Top. Curr. Chem.*, **132**, 63 (1986).

16) H. Imai and E. Kyuno, *Inorg. Chim. Acta*, **153**, 175 (1988).

17) R. M. Barrer, *J. Membr. Sci.*, **18**, 25 (1984).

18) G. H. Fredrickson and E. Helfand, *Macromolecules*, **18**, 2201 (1985).